ANALYSIS OF GEOMETRIC DEVIATION FEATURE INDUCED BY THE FDK FOR COMPUTED TOMOGRAPHY MEASUREMENTS

Lin XUE[1], Hiromasa SUZUKI[1], Yutaka OHTAKE[1], Hiroyuki FUJIMOTO[2], Makoto ABE[2], Osamu SATO[2], Toshiuuki TAKATSUJI[2]

1 RCAST, The University of Tokyo, 4-6-1, Komaba, Meguro, Tokyo 1538904, Japan, mechanicalautomaticxue@gmail.com
2 National Metrology Institute of Japan, National Institute of Advanced Industrial Science and Technology (AIST), Tsukuba, Ibaraki 305-8563, Japan

Abstract:
Recently, due to the ability to precisely measure inner and outer structure of a specimen in one single scan, X-ray computed tomography (CT) has entered the field of dimensional metrology in industry. Unfortunately, it is very difficult to realize industrial-level accuracy with CT for various factors. In this paper we analyze one of the most serious effects, the FDK (Feldkamp–Davis–Kress) effect, which can be observed in most of the common X-ray CT scanners with a cone beam. The FDK is the well-know reconstruction algorithm widely accepted as a standard reconstruction method for cone beam type of CT. However, this algorithm merely provides an approximate result, for the large dimension specimen, the FDK effect on measurement result is severe. Therefore, we aim at improving measurement accuracy by analyzing the geometric deviation induced by the single FDK effect. We conducted quantitative analysis on the FDK effect using numerical phantoms of the sphere and hole plate that are standard specimen for dimensional CT measurements. After discussing the cause of the FDK effect and the deviation distribution feature on different spatial positions for the chosen numerical phantoms, an improvement strategy of measurement accuracy is proposed.

Keywords: X-ray computed tomography, measurement accuracy, FDK, geometric deviation

1. INTRODUCTION

X-ray computed tomography (CT) is a well known technology in the medical community and in the field of material analysis and non-destructive testing and evaluation. Recently, as a new technology, X-ray CT has been broaden to the field of dimensional metrology [1]. In industry, dimensional metrology requires micron-level measurement accuracy. However, as CT is influenced by many factors, such as data processing, beam hardening, scattering, partial volume, etc. [2], the required accuracy is difficult to realize.

In order to promote the development of industrial computed tomography (ICT), a large number of studies have been done. Amirkhanov proposed a method for 3DCT scan positions optimization that is based on the analysis of Radon-space [3]. Kruth gave a detail report about the state of X-ray CT for dimensional quality control [1]. Schuetz et al. discussed strategies how to reduce the influence of environmental scattering in X-ray CT [4]. X-ray CT as a new technology for dimensional metrology has a very high potential, however, much development study is still necessary to make CT measurements reach maturity.

Figure (1) schematically illustrates ICT, showing that the main components are an X-ray source, a rotation table, and a detector. As a result of X-ray scanning, a sequence of 2D projection images of a specimen are obtained on the detector through rotation of the rotation table. Afterwards, the projection images are used to generate a CT volumetric model by a 3D reconstruction algorithm and an iso-surface mesh is extracted by a polygonization algorithm. Both 3D reconstruction and surface extraction affect CT measurement results. This paper aims at a numerical analysis of the 3D reconstruction effect on measurement accuracy and determining the deviation distribution feature induced by the 3D reconstruction effect.

Many different 3D reconstruction algorithms are available for cone beam tomography. The one most popular now for cone-beam ICT, owing to its easy implementation and high computation efficiency, is the FDK (Feldkamp–Davis–Kress) reconstruction algorithm [5]. This paper proposes a way to evaluate the FDK effect independently from other kinds of effects by use of CT simulation. By the analysis of reconstructed CT value, the cause of the FDK artifact is discussed. Then the geometric deviation on different spatial positions induced by the FDK effect is given.

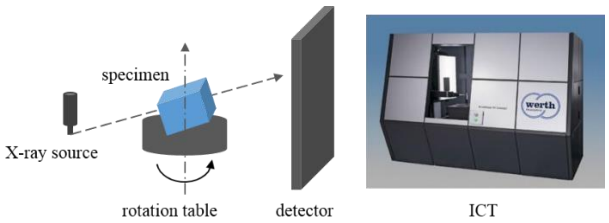

Fig. 1: Schematic of industrial computed tomography

2. METHOD OVERVIEW

2.1 Numerical Phantom

To evaluate geometric deviation induced by the FDK effect precisely, the numerical phantoms of the sphere and hole plate [see Fig. (2) (a) (b)] that are standard specimen for dimensional CT measurements are chosen as test objects in this research. In a practical CT reconstruction result, there are many kinds of artefacts. In order to separate the FDK artefact from other kinds of artefacts, we apply a simulation to take projection images without noise, thus the analysis of a single FDK effect can be realized. Note that as the detector

is discrete, the partial volume effect cannot be avoided. After ensuring proper computational efficiency, we make the size of detector pixel as small as possible to reduce the partial volume effect, and divide each detector pixel into as many small ones as possible to simulate the practical CT scan condition.

In this study, 600 projection images are taken in one 360° rotation, and different position parameters are used to obtain the simulation data of full spatial positions. Figure (2) (c) and (d) show the simulated 2D projection image of the numerical phantoms.

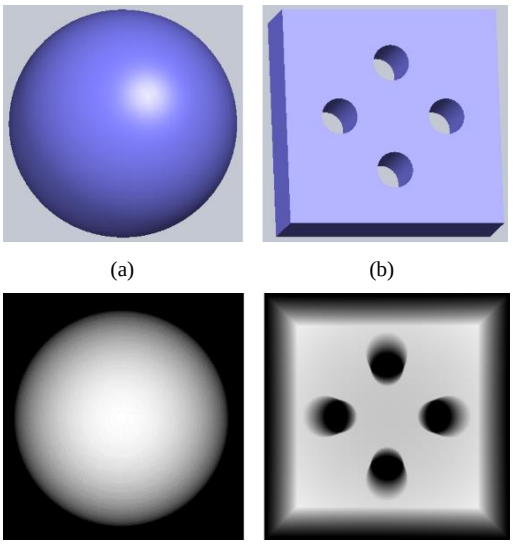

(a) (b)

(c) (d)

Fig. 2: Test phantom and simulated projection image. (a) sphere; (b) hole plate; (c) projection image of sphere; (d) projection image of hole plate

2.2 Analysis method

By the above method the projection images are produced to generate a CT volumetric model. Afterwards, CT polygonal meshes are computed from the volumetric model by use of the marching cubes algorithm [6]. In the process of surface extraction, the iso-surface global threshold value is used for edge detection. In this study, 0.6 is chosen as the CT value of the material and 0 is chosen as that of the background, so the threshold value is 0.3.

Now, common X-ray scanning methods are of two types, fan beam and cone beam. For the cone beam scanning, the algorithm used is known as the FDK method. In both cases, reconstruction of CT values is based on the filtered back projection (FBP) method. The CT value at a point in 3D space is computed by adding filtered projection values at points on the filtered projection images for all angles.

In fan beam reconstruction, the CT value at point M (Fig. (3)) can be obtained by summing the filtered projection values along the trajectory PM, which is a straight line on the projection plane. As this computation is theoretically accurate, CT values of voxels are accurate on the plane (focal plane) passing through the X-ray source and perpendicular to the axis of rotation. In cone beam reconstruction, the CT value at point N can be obtained by summing the filtered projection values along the trajectory PN, which is not a straight line but an elliptic path. Thus, the CT value of N is not accurate. The error increases with the increase in cone angle θ, and the error produces strong artifacts on the focal surface of an object. This phenomenon is called "the FDK effect". In practice, the cone angle is limited to small values to decrease the FDK effect.

In FDK data processing, compared with fan beam, only the scaling function along the vertical direction is added. Due to the similarity of the fan beam and the cone beam reconstruction algorithms, we compare the FDK algorithm with fan beam reconstruction algorithm in order to analyze the FDK effect.

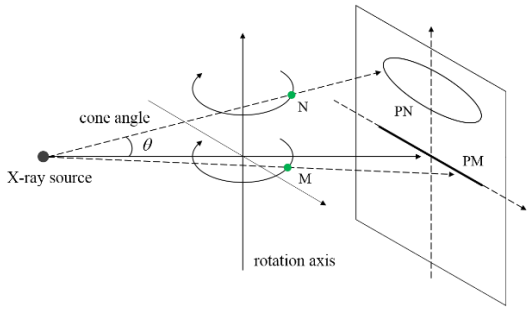

Fig. 3: Projection trajectory of fan beam scanning and cone beam scanning

3. DEVIATION DISTRIBUTION FEATURE

For small cone angles (about less than 6°), cone beam reconstruction can be approximated as fan beam reconstruction, resulting in very small deviation. As the cone angle increases, the reconstruction deviation likewise increases. To observe the deviation distribution induced by the FDK clearly, we analyze the FDK effect for a large cone angle.

3.1 Sphere

We first place a sphere on the table with its center on the origin. Figure (4) shows the arrangement of CT coordinate system and a sphere. The Z axis of the coordinate system is defined to be the same as the axis of rotation. The origin is located at the intersection point of the Z axis and the focal plane. Then the X axis is defined to be a line connecting the x-ray focus and the origin. The Y axis is defined as the third axis perpendicular to the X and Z axes.

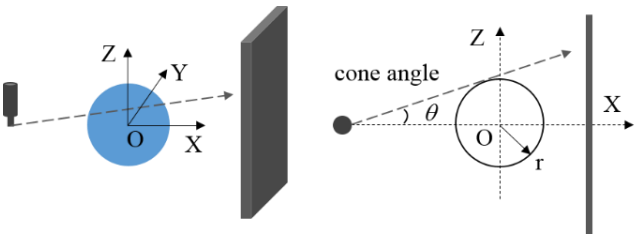

Fig. 4: CT coordinate system with a sphere

Figure (5) shows the simulation result of a sphere. The resolution of the reconstructed model is 362x362x360. Figure (5) (a) shows an iso-surface with color distribution of geometric deviation. It is observed that the deviation around the poles is so large that the surface is inflated sharply

around the poles. The CT slice image (XZ slice) is shown in Fig. (5) (b). In the top and bottom poles, CT values outside the sphere should be zero as there exists no material. But due to the FDK effect, in FDK reconstruction as all the scaled projection values are close to the projection values for a fan beam, all the CT values are not far from correct ones. As shown in Fig. (5) (c), the CT values in these shade areas around the poles (see Fig. (5) (b)) are not zero but greater than the threshold value. Such non-zero CT values in these shade areas cause large geometric deviation to the iso-surface. And with increases in the shade areas, the geometric deviation likewise increases.

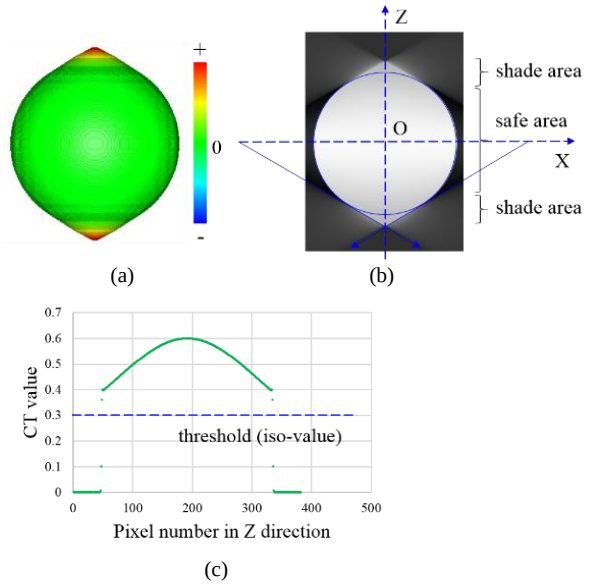

Fig. 5: Deviation generation for a sphere (r=25, pixel size=0.2, cone angle=30°). (a) reconstructed CT model; (b) reconstructed slice (XZ slice); (c) CT value profile along the Z axis

Figure (6) shows the geometric deviation distribution of a sphere after movement. It is observed that the geometric deviation on the area around the top pole increases after movement along the Z axis. And for the case of movement along the X axis, the surface with large geometric deviation moves after movement.

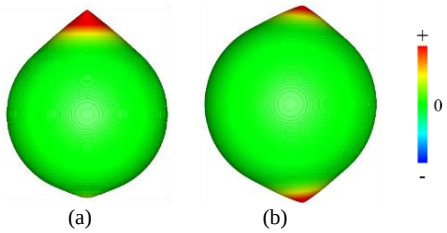

Fig. 6: Positional effects for a sphere. (a) movement along the Z axis; (b) movement along the X axis

On the other hand, the deviation in most of the surface area outside the shade areas is quite small and some is close to 0. We call this area "safe area". It is reasonable to measure the sphere by using the iso-surface in the safe area. We compute the radius of the sphere by fitting a sphere in the safe area in the following positional effects analysis. Here least square fitting is used and the safe area is chosen to be as large as possible not to overlap the shade areas.

We analyze the FDK effect on the measurement of a sphere in all spatial positions by moving sphere along the X and Z axes. As shown by Fig. (7), for both cases, the radius error is nearly the same at all positions and sufficiently small after movement. In summary, we can conclude that though the geometric deviation induced by the FDK effect changes after movement, there is nearly no change in the radius error of a sphere by fitting a sphere in the safe area. However, as the shade areas with large geometric deviation change after movement, the sphere had better be placed around the origin.

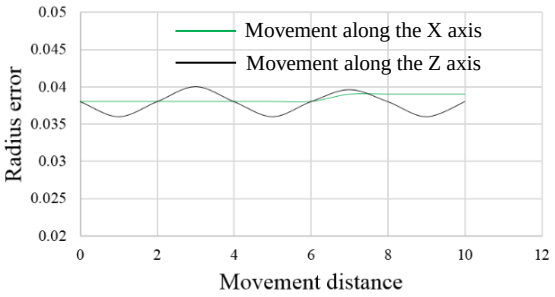

Fig. 7: Positional effects for a sphere (r=25, pixel size=0.2, cone angle=30°)

3.2 Hole Plate

Hole plate consists of cylindrical holes and cuboid that have a similar geometric feature. The geometric feature of cylinder and cuboid is identical along the central axis. And as cube has a special size among cuboids, in this part we first show numerical analysis of a cube.

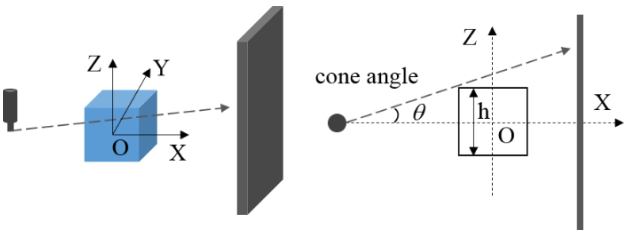

Fig. 8: CT coordinate system with a cube

First a cube without slant angle is placed on the table with its center on the origin (see Fig. (8)). Figure (9) shows the simulation result. The resolution of the reconstructed model is 366x366x366. Figure (9) (a) shows an iso-surface with color distribution of geometric deviation. Here the two planes perpendicular to the Z axis are defined to be plane A, the two planes perpendicular to the X axis are defined to be plane B, and the others are defined to be plane C. It is observed that plane A suffers from severe FDK effect. The geometric deviation on plane A is large and plane A is concave. The geometric deviation on plane B and C are much smaller than that on plane A. Figure (9) (b) shows a XZ reconstructed slice that passes the Z axis. In area a, as all the scaled projection values are much smaller than the projection values for a fan beam, the CT values are much smaller than correct ones. A CT value profile along line k

(see Fig. (9) (b)) that locates on the actual position of plane A is shown in Fig. (9) (c). It is observed that all the CT values are smaller than correct ones and most are smaller than the threshold value, so the FDK effect on plane A is severe and plane A is concave. In area c, for the area near the surface of the cube, as the scaled projection values are close to the projection values for a fan beam, the CT values are close to correct and the deviation on this surface is close to 0. And the CT values of the area around the Z axis in area c are correct. In area b, the scaled projection values have features of those in both area a and c, so the CT values become slightly smaller than correct ones, resulting in small deviation on the surface.

In summary, for the case of the cube, we can conclude that the FDK effect is severe in areas for which the scaled projection values for a cone beam differ greatly from the projection values for a fan beam.

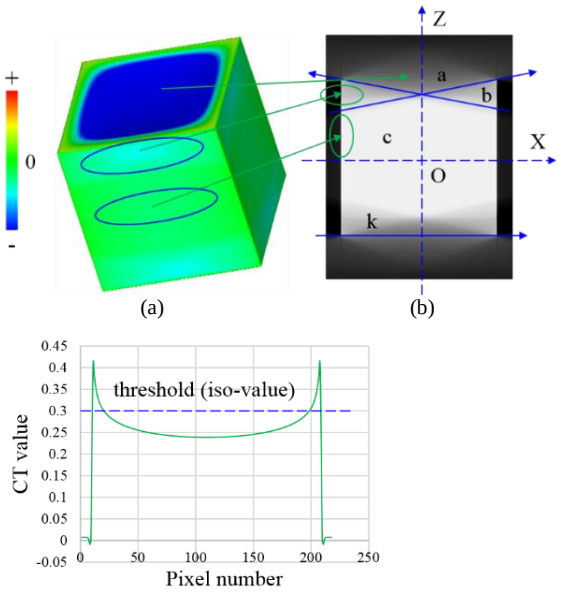

(c)

Fig. 9: Deviation generation for a cube (h=60, pixel size=0.3, cone angle=23.2°). (a) reconstructed CT model; (b) reconstructed slice (XZ slice); (c) CT value profile along line k

Figure (10) shows the geometric deviation distribution of a cube after movement. Compared with the case of without movement, the maximum geometric deviation increases after movement along the Z axis. For the case of movement along the X axis, it is observed that the surface with large geometric deviation moves after movement.

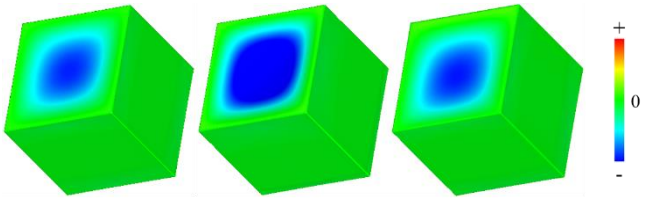

(a) (b) (c)

Fig. 10: Positional effects for a cube. (a) without movement; (b) movement along the Z axis; (c) movement along the X axis

We analyse the FDK effect on the measurement of a cube in all spatial positions by moving cube along the X and Z axes and slanting cube around the Y axis. We use least square fitting to fit six planes in the areas of each plane, and the height is computed as the distance between two parallel planes, then compare the value with the true one to evaluate the dimensional error. Here the distance error between the two planes perpendicular to the Z axis is defined to be height error A, the distance error between the two planes perpendicular to the X axis is defined to be height error B, and the distance error between the two planes perpendicular to the Y axis is defined to be height error C.

For the case of movement along the X and Z axes, as shown by Fig. (11), the height error is nearly the same at all positions. It is observed that the height error A is large. On the other hand, the height error B and C is sufficiently small.

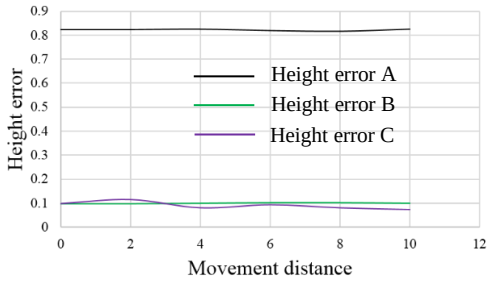

(a)

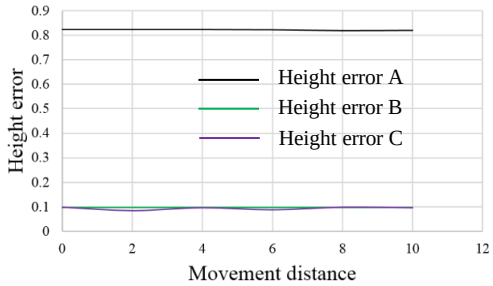

(b)

Fig. 11: Positional effects for a cube (h=30, pixel size=0.2, cone angle=18.4°). (a) movement along the X axis; (b) movement along the Z axis

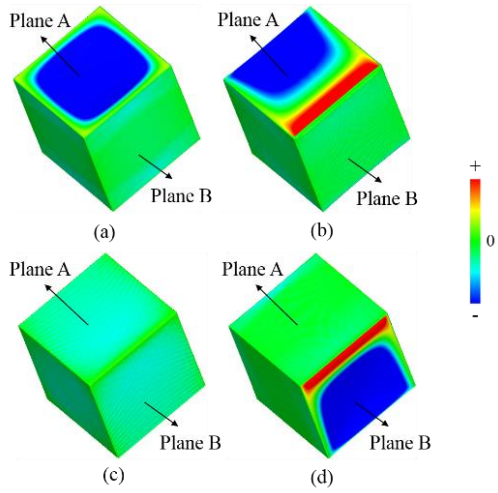

Fig. 12: Geometric deviation distribution of a cube with different slant angle ϕ. (a) ϕ=0°; (b) $\phi < \beta$; (c) $\beta < \phi < \gamma$; (d) $\phi > \gamma$

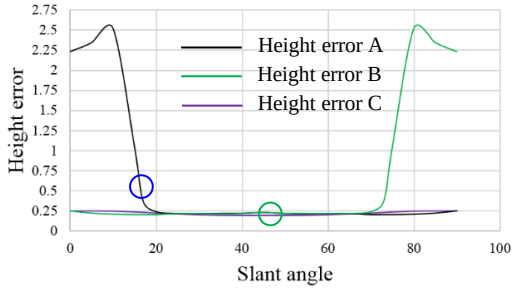

Fig. 13: Positional effects for a cube slanted around the Y axis (h=60, pixel size=0.3, cone angle=23.2°)

For the case of a cube slanted around the Y axis, Figure (12) shows the geometric deviation distribution of a cube with different slant angles. Among the slant angles, there are two special angles, β and γ. β represents the position at which the X-rays are tangent to plane A. γ represents the position at which the X axis coincides with the diagonal of the XZ section of the cube, for a cube, γ is 45°. It is obvious that the geometric deviation on all the planes is small in the case of slant angle ϕ satisfying $\beta < \phi < \gamma$. In this case, the scaled projection values become close to the projection values for a fan beam, resulting in decreased deviation compared with the other cases. It is noticed that with ϕ close to 90°, the FDK effect on plane B is severe, resulting in a large deviation on plane B. For the case of slant angle $\phi < \beta$, in some area on plane A, the CT values become smaller than the case without a slant angle, resulting in increased deviation and movement of the position with maximum deviation. The height error computed by fitting plane is shown in Fig. (13). The blue circle indicates the position of β and the green one indicates the position of γ. We can conclude that when the cube is slanted at an angle from about $\gamma - \mu$ to γ degrees, the fair measurement accuracy of height for each plane can be obtained, and that measurement at a smaller slant angle is not recommended. The value of μ depends on the size of a cube, here it is about 15°.

As a cylinder and a cube have similar geometric feature along the central axis for cone beam scanning, their geometric deviation distribution induced by the FDK effect is similar. As shown in Fig. (14), β represents the position at which the X-rays are tangent to the top surface of the cylinder and γ represents the position at which the X axis coincides with the diagonal of the XZ section of the cylinder. It is observed that the geometric deviation on the cylinder is similar with that on the cube in the case of different slant angles. The height error computed by fitting plane and the radius error computed by fitting cylinder are shown in Fig. (15). The blue circle and the green circle indicate the position of β and γ respectively. We can conclude that when the cylinder is slanted at an angle larger than about $\gamma - \mu$ degrees, the fair measurement accuracy of height can be obtained. μ depends on the size of a cylinder, here it is about 10°. In the case of radius error, we can conclude that when the cylinder is slanted at an angle smaller than γ degrees, the high measurement accuracy can be obtained. It is noticed that in the case of slant angle larger than γ degrees, though the deviation on the cylindrical surface is large, the radius error is sufficiently small by choosing points with small deviation in the safe area to fit a cylinder.

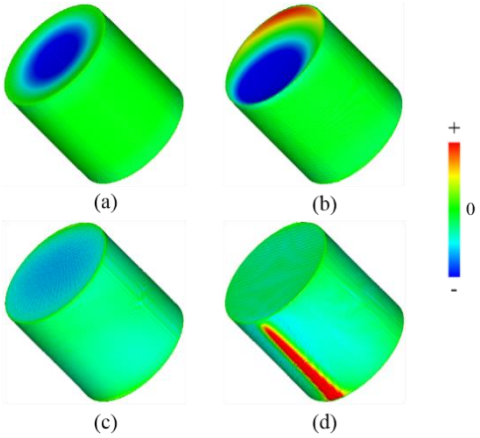

Fig. 14: Geometric deviation distribution of a cylinder with different slant angle ϕ. (a) ϕ=0°; (b) $\phi < \beta$; (c) $\beta < \phi < \gamma$; (d) $\phi > \gamma$

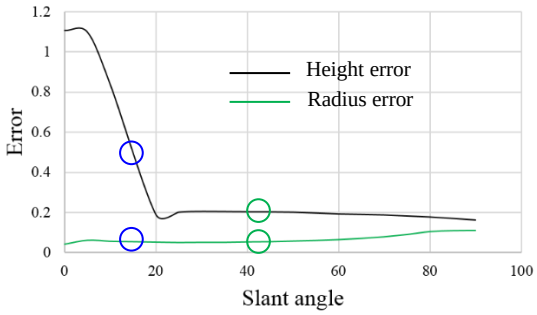

Fig. 15: Positional effects for a cylinder slanted around the Y axis (cylinder height=50, cylinder radius=25, pixel size=0.3, cone angle=18°)

Further, the geometric deviation distribution of the hole plate is described. The hole plate model used in this study consists of four cylindrical holes and a cuboid. Figure (16) shows the geometric structure of the hole plate placed with its center on the origin. Two planes with cylindrical holes are perpendicular to the Z axis. Cylindrical hole R1 and R4 are symmetric with respect to the XZ plane and cylindrical hole R2 and R3 are symmetric with respect to the YZ plane. As shown in Fig. (17), though the geometric structure of the hole plate is complex, the geometric deviation distribution induced by the FDK effect is similar to that of a cube and a cylinder.

Due to the symmetry, the measurement result of R1 and R2 is the same with that of R4 and R3 respectively. Here we show the radius error of R1 and R2 and the height error between the two planes perpendicular to the Z axis. The height error computed by fitting plane and the radius error computed by fitting cylinder are shown in Fig. (18). Compared with the cases of a cube and a cylinder, in the hole plate, there is slight change in the geometrical features, resulting in a little change in the error. Therefore, the conclusions for a cube and a cylinder are applicable to those for the hole plate.

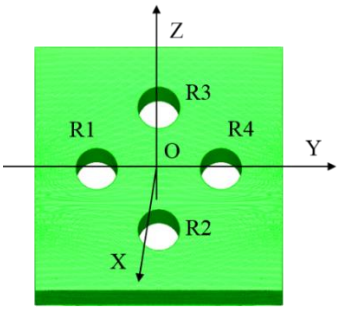

Fig. 16: Positional parameters of hole plate

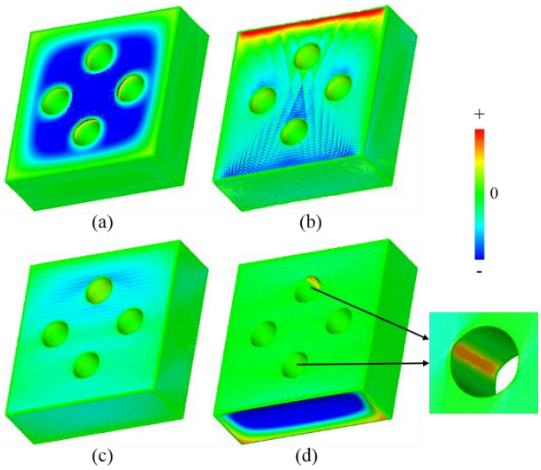

Fig. 17: Geometric deviation distribution of a hole plate with different slant angle ϕ. (a) ϕ=0°; (b) $\phi < \beta$; (c) $\beta < \phi < \gamma$; (d) $\phi > \gamma$

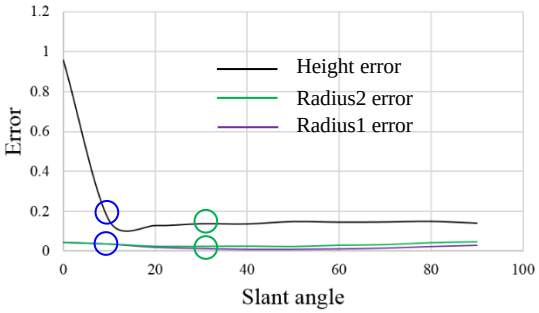

Fig. 18: Positional effects for a hole plate slanted around the Y axis (height between the two planes perpendicular to the Z axis =20, radius=5, pixel size=0.2)

4. CONCLUSION AND FUTURE WORK

This paper gives a detailed description of the geometric deviation feature induced by the FDK effect by use of a sphere and a hole plate. Based on the proposed method, the geometric deviation feature of different objects induced by the FDK effect can be evaluated. By analyzing measurement error on different spatial positions, a method for improving measurement accuracy is given. In future work, we plan to evaluate the FDK effect on some other standard specimens with complex shapes so that the method can be applied to a wide range of shapes and objects.

REFERENCES

[1] J. P. Kruth. Computed tomography for dimensional metrology. CIRP Annals-Manufacturing Technology 60: 821–842, 2011.

[2] F. Welkenhuyzen, 2009, OPTIME. Industrial Computer Tomography for Dimensional Metrology: Overview of Influence Factors and Improvement Strategies.

[3] Artem Amirkhanov. Visual Optimality and Stability Analysis of 3DCT Scan Positions. IEEE Computer Society, VOL. 16, NO. 6, pages 1477-1486, 2010.

[4] Philipp Schuetz, 2012, ICT. Strategies for the reduction of environmental scattering in X-ray Computed Tomography.

[5] L. A. Feldkamp, 1984. Practical cone-beam algorithm. JOSA A, Vol. 1, Issue 6, pp. 612–619.

[6] W. E. Lorensen, 1987. Marching cubes: a high resolution 3d surface construction algorithm. Proc. ACM Siggraph, '87, pp 163-169.